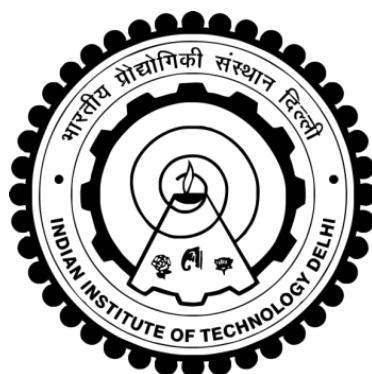


**DEVELOPMENT OF NANOSTRUCTURED MATERIALS
FOR PHOTOELECTROCHEMICAL AND FUEL CELL
APPLICATIONS**

NIMAI BHANDARY



**DEPARTMENT OF CHEMISTRY
INDIAN INSTITUTE OF TECHNOLOGY DELHI
OCTOBER 2018**

©Indian Institute of Technology Delhi (IITD), New Delhi, 2018

**DEVELOPMENT OF NANOSTRUCTURED MATERIALS
FOR PHOTOELECTROCHEMICAL AND FUEL CELL
APPLICATIONS**

by

NIMAI BHANDARY

DEPARTMENT OF CHEMISTRY

Submitted

In fulfilment of the requirements of the degree of Doctor of Philosophy

to the



INDIAN INSTITUTE OF TECHNOLOGY DELHI

OCTOBER 2018

DEDICATE TO ALL MY TEACHERS

Certificate

It is certified that the thesis entitled “**Development of Nanostructured Materials for Photoelectrochemical and Fuel Cell Application**” being submitted by **Mr. Nimai Bhandary** to the Department of Chemistry, Indian Institute of Technology Delhi for the award of the degree of **Doctor of Philosophy** in Chemistry, is a record of bonafide research work carried out by him. Mr Nimai Bhandary has worked under our supervision and has fulfilled all the requirements for submission of this thesis, which to our knowledge has reached the requisite standard.

The results contained in this thesis have not been submitted to any other university or institute either in part or full for the awards of any other degree or diploma.

Dr. Pravin P. Ingole
Assistant Professor
Department of Chemistry
Indian Institute of Technology Delhi

Prof. Suddhasatwa Basu
Professor
Department of Chemical Engineering
Indian Institute of Technology Delhi

Acknowledgements

First of all, I would like to express my gratitude for my PhD supervisors Dr. Pravin P. Ingole and Professor Suddhasatwa Basu; they are incredible mentors throughout my research tenure. I am highly motivated to continue research for their excellent guidance, constant encouragement, caring and wholehearted cooperation during stages of my work. Their gigantic knowledge of the subject has helped me in understanding various aspects of electrochemistry area. I am very much grateful for their kind support and proud of being their student. I would like to thank my research committee members; Prof. A. Ramanan, Prof. Shasank Deep and Prof. Anupam Shukla for their valuable suggestion to improve my research work.

I would like to thank Prof. A. K. Ganguly Head, Department of Chemistry and all other faculty members for their help and assistance during my PhD programme. It is high time to express my gratitude to my lab members specially Dr. Aadesh P Singh, (simply an awesome personality) Dr. Pankaj Tiwari (always happy to help), Mr. Harikrishnan (never reluctant to help), Mr. Ravi, other colleagues from Chemistry lab and specially Mr. Sundar Singh for their immense support on me during my research. I could not have far better colleagues than them who helped me a lot whenever I required. I'd like to thank all the staff members from Department of Chemistry for their support during my research tenure.

I owe my existence to the meticulous care and love of my parents, brother and sisters. They have always sacrificed their own wishes and happiness for uplifting of my career.

I bow down in front of God for providing me the health, strength and this opportunity in my life

--Nimai Bhandary

Abstract

Renewable energy sources are currently fastest growing energy solution to compensate the ever increasing energy consumption demands. The utilization of solar energy as an alternative to conventional energy source has drawn much attention since last few decades. Storing of solar energy in the form of chemical bond like hydrogen has been given much importance recently. Additionally, fuel cell is also an area of immense importance to meet future energy demands. The thesis is aimed to synthesize and characterize various nanostructured materials by simple method such as electrodeposition or chemical route for application in photoelectrochemical (PEC) water splitting and oxygen reduction reaction catalyst for alkaline fuel cell. These two areas have immense potential to meet the future energy demands. Primarily, it is important to design an efficient electrocatalyst which will work effectively to meet the criteria for the applications in commercial purpose and which will be stable for long duration at the same time. In this direction, the thesis reports synthesis of semiconductor materials such as hematite ($\alpha\text{-Fe}_2\text{O}_3$) and graphitic carbon nitride ($\text{g-C}_3\text{N}_4$) by simple electrodeposition and solid state heat treatment procedures. The surface passivation of hematite ($\alpha\text{-Fe}_2\text{O}_3$) photoanodes by an oxygen evolution reaction (OER) co-catalyst NiMnOx results in enhanced photocurrent density. Solar photo conversion efficiency (STH) is achieved upto 0.85% for modified hematite photoanode with 200s NiMnOx layer. Next, in-situ solid state synthesis of bimetallic AgNi incorporated graphitic carbon nitride by simple heat treatment in N_2 atmosphere is reported for PEC water splitting and Rhodamine B dye degradation. These metal nanoparticles incorporated photoelectrodes demonstrate improved photoactivity due to faster charge transport. The photocurrent density increases upto 1.2 mA/cm^2 and the maximum dye degradation efficiency achieved is upto 95%. Further work is carried out

on electrochemical modification of hematite dendrites/carbon nitride composite by CoFeO_x co-catalyst for application in PEC water splitting. The said heterojunction leads to improved PEC activity with 0.60 mA/cm² photocurrent density at 1.23 V vs. RHE. The work on development of electrocatalyst for oxygen reduction reaction (ORR) in alkaline medium is carried out in search of better cathode catalyst in alkaline fuel cell. Here one step electrodeposition of AgCd electrocatalyst on carbon paper for ORR application is reported. The ORR is found to follow four electron pathways. Next, ORR study of Ag incorporated g-C₃N₄ material supported on graphene oxide synthesized by solid state heat treatment route is also investigated in alkaline medium. The ORR study reveals that it follows most favourable four electrons pathway. Following the chapters in details, the thesis present conclusion and future scope where a device fabrication combining PEC and fuel cell is suggested for application in commercial purpose with developed catalysts.

सार

नवीकरणीय ऊर्जा स्रोत वर्तमान में बढ़ती ऊर्जा खपत मांगों की भरपाई करने के लिए सबसे तेजी से बढ़ रहे ऊर्जा समाधान हैं। पारंपरिक ऊर्जा स्रोत के विकल्प के रूप में सौर ऊर्जा के उपयोग ने पिछले कुछ दशकों से काफी ध्यान आकर्षित किया है। हाइड्रोजन जैसे रासायनिक बंधन के रूप में सौर ऊर्जा का भंडारण हाल ही में बहुत महत्व दिया गया है। इसके अतिरिक्त, ईंधन सेल भी भविष्य की ऊर्जा मांगों को पूरा करने के लिए अत्यधिक महत्व का एक क्षेत्र है। थीसिस का लक्ष्य विभिन्न प्रकार के नैनोस्ट्रक्चर सामग्री को सरल तरीके से संश्लेषित करना और विशेषता करना है जैसे इलेक्ट्रोडोपेशन या फोटोइलेक्ट्रोकेमिकल (पीईसी) पानी विभाजन में अनुप्रयोग के लिए रासायनिक मार्ग और क्षारीय ईंधन सेल के लिए ऑक्सीजन कमी प्रतिक्रिया उत्प्रेरक। इन दोनों क्षेत्रों में भविष्य की ऊर्जा मांगों को पूरा करने की अत्यधिक संभावना है। मुख्य रूप से, एक कुशल इलेक्ट्रोकाटिस्टिस्ट को डिजाइन करना महत्वपूर्ण है जो वाणिज्यिक उद्देश्यों में अनुप्रयोगों के मानदंडों को पूरा करने के लिए प्रभावी ढंग से काम करेगा और जो एक ही समय में लंबी अवधि के लिए स्थिर रहेगा। इस दिशा में, थीसिस इलेक्ट्रोडोशन और ठोस राज्य ताप उपचार प्रक्रियाओं द्वारा अर्धचालक पदार्थ जैसे हेमेटाइट ($\alpha\text{-Fe}_2\text{O}_3$) और ग्राफिक कार्बन नाइट्राइड ($\text{g-C}_3\text{N}_4$) के संश्लेषण की रिपोर्ट करता है। ऑक्सीजन विकास प्रतिक्रिया (ओईआर) सह-उत्प्रेरक NiMnO_x द्वारा हेमेटाइट ($\alpha\text{-Fe}_2\text{O}_3$) फोटोनोड्स की सतह निष्क्रियता में वृद्धि हुई फोटोकुरेंट घनत्व में परिणाम होता है। 200s फोटो NiMnO_x परत के साथ संशोधित हेमेटाइट फोटोनोड के लिए सौर फोटो रूपांतरण दक्षता (एसटीएच) 0.85% तक हासिल की जाती है। इसके बाद, पीईसी जल विभाजन और रोडोमाइन बी डाई गिरावट के लिए एन 2 वायुमंडल में सरल गर्मी उपचार द्वारा द्विपक्षीय एग्नी के ग्राउंडिटिक कार्बन नाइट्राइड में अंतर्निहित ठोस राज्य संश्लेषण की सूचना दी गई है। इन धातु नैनोकणों में शामिल फोटोइलेक्ट्रोड तेजी से चार्ज परिवहन के कारण बेहतर फोटोएक्टिविटी का प्रदर्शन करते हैं। फोटोकुरेंट घनत्व 1.2 एमए / सेमी² तक बढ़ता है और अधिकतम डाई गिरावट दक्षता 95% तक बढ़ जाती है। पीईसी जल

विभाजन में आवेदन के लिए CoFeO_x सह-उत्प्रेरक द्वारा हेमेटाइट डेंड्राइट / कार्बन नाइट्राइड समग्र के इलेक्ट्रोकेमिकल संशोधन पर आगे का काम किया जाता है। कहा गया हेटरोजंक्शन 1.23 V बनाम आरएचई पर 0.60 एमए / सेमी^2 फोटोकुरेंट घनत्व के साथ पीईसी गतिविधि में सुधार की ओर जाता है। क्षारीय माध्यम में ऑक्सीजन कमी प्रतिक्रिया (ओआरआर) के लिए इलेक्ट्रोक्ैटालिस्ट के विकास पर कार्य क्षारीय ईंधन सेल में बेहतर कैथोड उत्प्रेरक की खोज में किया जाता है। ओआरआर आवेदन के लिए कार्बन पेपर पर एजीसीडी इलेक्ट्रोक्ैटालिस्ट की एक कदम इलेक्ट्रोडोपाइजेशन की सूचना दी गई है। ओआरआर चार इलेक्ट्रॉन मार्गों का पालन करने के लिए पाया जाता है। इसके बाद, ठोस राज्य गर्मी उपचार मार्ग द्वारा संश्लेषित ग्रैफेन ऑक्साइड पर समर्थित एजी शामिल $g\text{-C}_3\text{N}_4$ सामग्री का ओआरआर अध्ययन भी क्षारीय माध्यम में जांच की जाती है। ओआरआर अध्ययन से पता चलता है कि यह सबसे अनुकूल चार इलेक्ट्रॉन मार्ग का पालन करता है। विवरण में अध्यायों के बाद, थीसिस वर्तमान निष्कर्ष और भविष्य के दायरे जहां विकसित उत्प्रेरक के साथ व्यावसायिक उद्देश्य में आवेदन के लिए पीईसी और ईंधन सेल का संयोजन करने वाला उपकरण निर्माण सुझाव दिया जाता है।

List of Contents

Certificate.....	i
Acknowledgements.....	ii
Abstract.....	iii
Abstract (in Hindi).....	v
List of content.....	vii
List of figures.....	x
List of tables.....	xvi
List of abbreviations and symbols.....	xvii
CHAPTER 1 Introduction	
1.1 Global Energy Scenario: Role of PEC cell and Fuel Cell.....	1
1.2 Concept of Photoelectrochemical cell.....	3
1.3 Semiconductor Materials.....	4
1.4 Semiconductor Modifications.....	6
1.5 Principles of Fuel Cell.....	9
1.6 Types of Fuel Cell.....	10
1.7 ORR in Alkaline Fuel Cell.....	12
1.8 Electrocatalyst for ORR.....	13
1.9 Electrode fabrication for PEC measurements.....	14
1.10 Mott-Schottky Analysis.....	15
1.11 Cyclic Voltammetry.....	17
1.12 Rotating ring disk electrode (RRDE) voltammetry	18
1.13 In-situ FTIR spectroscopy.....	20
1.14 Scope of this thesis.....	20
1.15 References.....	21

CHAPTER 2 Enhanced photoelectrochemical performances of electrodeposited hematite films decorated with nanostructured NiMnO_x

2.1	Abstract.....	24
2.2	Introduction.....	30
2.3	Experimental Section.....	26
2.4	Results and Discussion.....	29
2.5	Conclusion.....	42
2.6	References.....	43

CHAPTER 3 In-situ solid state synthesis of AgNi/g-C₃N₄ nanocomposite for enhanced photoelectrochemical and photocatalytic activity

3.1	Abstract.....	46
3.2	Introduction.....	46
3.3	Experimental Section.....	49
3.4	Results and Discussion.....	51
3.5	Conclusions.....	67
3.6	References.....	68

CHAPTER 4 Enhanced photoelectrochemical performance of CoFeO_x sensitized hematite dendrites/g-C₃N₄ nanocomposite

4.1	Abstract.....	70
4.2	Introduction.....	71
4.3	Experimental Section.....	72
4.4	Results and Discussion.....	73
4.5	Conclusions.....	83

4.6	References.....	84
-----	-----------------	----

CHAPTER 5 Single step fabrication of nano-flakes like AgCd alloy electro-catalyst for oxygen reduction reaction in alkaline fuel cell

5.1	Abstract.....	86
5.2	Introduction.....	87
5.3	Experimental Section.....	89
5.4	Results and Discussion.....	91
5.5	Conclusions.....	102
5.6	References.....	103

CHAPTER 6 A noble-metal-free Ag/g-C₃N₄@GO nanocomposite based efficient electrocatalyst for oxygen reduction reaction in alkaline fuel cell

6.1	Abstract.....	106
6.2	Introduction.....	107
6.3	Experimental Section.....	109
6.4	Results and Discussion.....	112
6.5	Conclusions.....	125
6.6	References.....	126

CHAPTER 7 Conclusion and Future Prospects.....128

List of Figures

Figure 1.1 World energy consumption by countries (in quadrillion Btu) (left) and total energy consumption by energy sources (in quadrillion Btu).....	2
Figure 1.2 Basic configuration of PEC cell.....	4
Figure.1.3 Band edge position of semiconductors used for PEC water splitting	5
Figure 1.4 Band edge position of ideal semiconductor.....	6
Figure 1.5 Types of semiconductor with different band edge position	7
Figure 1.6 Schematic of fuel cell.....	10
Figure 1.7 Digital image of a fabricated working electrode.....	14
Figure 1.8 Digital image of Teflon made PEC cell.....	15
Figure 1.9 A Mott-Schottky figure showing flatband potential and slope.....	16
Figure 1.10 Cyclic voltammetry for a reversible system.....	18
Figure 1.11 Digital image of RRDE electrode tip.....	19
Figure 2.1 XRD patterns of (a) pristine α -Fe ₂ O ₃ and (b) NiMnO _x loaded α -Fe ₂ O ₃ for different deposition time.....	29
Figure 2.2 Raman spectra for (a) pristine α -Fe ₂ O ₃ and (b) 200s NiMnO _x loaded on α -Fe ₂ O ₃ by electrodeposition technique.....	30
Figure 2.3 FE-SEM images of (a) pristine α -Fe ₂ O ₃ ; and (b) 200s NiMnO _x loaded α -Fe ₂ O ₃ by electrodeposition technique.....	31

Figure 2.4 Optical absorption spectra for pristine and NiMnO _x loaded α -Fe ₂ O ₃ for different electrodeposition time.....	32
Figure 2.5 XPS spectra of pristine and 200s NiMnO _x deposited α -Fe ₂ O ₃ for (a) Fe 2 <i>p</i> (b) O 1 <i>s</i> (c) Mn 2 <i>p</i> and (d) (c) Ni 2 <i>p</i> in 200s NiMnO _x deposited α -Fe ₂ O ₃ sample.....	33
Figure 2.6 EDX analysis of (a) pristine α -Fe ₂ O ₃ ; and (b) 200s NiMnO _x loaded α -Fe ₂ O ₃	34
Figure 2.7 (a) Photoelectrochemical performances in terms of current–potential curves for α -Fe ₂ O ₃ and NiMnO _x deposited α -Fe ₂ O ₃ photoanodes in 1M NaOH (pH = 13.6) solution. (b) Photoconversion efficiency versus applied potential curves for α -Fe ₂ O ₃ and NiMnO _x deposited α -Fe ₂ O ₃ photoanodes.....	34
Figure 2.8 Mott–Schottky plots of pristine α -Fe ₂ O ₃ and NiMnO _x loaded α -Fe ₂ O ₃ photoanode for various electrodeposition times.....	37
Figure 2.9 Nyquist plots of electrochemical impedance spectra of pristine α -Fe ₂ O ₃ and NiMnO _x loaded α -Fe ₂ O ₃ photoanode for various deposition time under visible light illumination.....	39
Figure 2.10 Photoluminescence spectra of (a) pristine α -Fe ₂ O ₃ and (a) 200s NiMnO _x deposited α -Fe ₂ O ₃ photoanode.....	40
Figure 2.11 Schematic representation of energy level band alignments between α -Fe ₂ O ₃ and NiMnO _x in (a) electrolyte and (b) the formation of p–n junction in electrolyte.....	41
Figure 3.1 (a) PXRD pattern of g-C ₃ N ₄ and metal doped g-C ₃ N ₄ ; (b) Enlarged portion of maximum intense peak and (c) Enlarged portion from 35° to 50° 2-theta values.....	52

Figure 3.2 (a) UV-Vis diffuse reflectance spectra and (b) Kubelka–Munk function versus the energy plot of g-C ₃ N ₄ , Ni-g-C ₃ N ₄ , and Ag/g-C ₃ N ₄ and AgNi/g-C ₃ N ₄	53
Figure 3.3 (a) FTIR spectra of g-C ₃ N ₄ and metal embedded g-C ₃ N ₄	54
Figure 3.4 SEM images of pure (a) g-C ₃ N ₄ (b) AgNi/g-C ₃ N ₄ and (c-f) elemental mapping of AgNi/g-C ₃ N ₄ catalyst showing distribution of C, N, Ni and Ag.....	55
Figure 3.5 TEM images of (a) pure g-C ₃ N ₄ and (b) AgNi/g-C ₃ N ₄ . EDAX spectra of (c) pure g-C ₃ N ₄ and (d) for AgNi/g-C ₃ N ₄	56
Figure 3.6 Photoelectrochemical performances in terms of current–potential curves for g-C ₃ N ₄ , Ni-g-C ₃ N ₄ , and Ag/g-C ₃ N ₄ and AgNi/g-C ₃ N ₄	59
Figure 3.7 Mott-Schottky plots under dark condition for g-C ₃ N ₄ , Ni-g-C ₃ N ₄ , and Ag/g-C ₃ N ₄ and AgNi/g-C ₃ N ₄	60
Figure 3.8 (a) Nyquist plots for g-C ₃ N ₄ , Ni-g-C ₃ N ₄ , and Ag/g-C ₃ N ₄ and AgNi/g-C ₃ N ₄ ; (b) Bode plots for g-C ₃ N ₄ and AgNi/g-C ₃ N ₄	61
Figure 3.9 (a) Photocatalytic degradation of g-C ₃ N ₄ , Ni/g-C ₃ N ₄ , Ag/g-C ₃ N ₄ , and AgNi/g-C ₃ N ₄ . (Inset shows colour change after dye degradation in 90 minutes). (b) Degradation efficiency of g-C ₃ N ₄ , Ag/g-C ₃ N ₄ , Ni/g-C ₃ N ₄ and AgNi/g-C ₃ N ₄ photocatalyst for the degradation of RhB solution.....	63
Figure 3.10 Plot of ln(C ₀ /C) as a function of visible irradiation time for photocatalysis of RhB solution containing: g-C ₃ N ₄ , Ni/g-C ₃ N ₄ , Ag/g-C ₃ N ₄ , and AgNi/g-C ₃ N ₄ under visible light irradiation.....	64
Figure 3.11 Oxygen-reduction reaction of g-C ₃ N ₄ , Ni/g-C ₃ N ₄ , Ag/g-C ₃ N ₄ and AgNi/g-C ₃ N ₄	65

Figure 3.12 Proposed mechanistic scheme for dye degradation of AgNi/g-C ₃ N ₄ photocatalyst.....	66
Figure 4.1 FESEM images of (a) HD, (b) HD-CN, (c) CoFeO _x /HD-CN and (d) Enlarged portion of (c).....	75
Figure 4.2 XRD pattern of (a) HD, (b) HD-CN and (c) CoFeO _x /HD-CN.....	76
Figure 4.3 Raman spectra for (a) HD and (b) HD-CN and (c) CoFeO _x deposited on HD.....	77
Figure 4.4 EDX analysis of CoFeO _x /HD-CN.....	78
Figure 4.5 Photoelectrochemical performances in term of current–potential curve for HD, HD-CN and CoFeO _x /HD-CN.....	79
Figure 4.6 Mott-Schottky plots for (a) HD and HD-CN and (b) CoFeO _x /HD-CN.....	80
Figure 4.7 EIS analysis of HD, HD-CN and CoFeO _x /HD-CN.....	82
Figure 4.8 Possible mechanistic scheme for the heterojunction.....	83
Figure 5.1 XRD pattern of carbon paper (a) before and (b) after AgCd particles have been electro-deposited.....	92
Figure 5.2 SEM images of (a) carbon paper and (b) AgCd elctro-deposited on carbon paper, (c) Higher magnifications of the image of (b) with nanoflakes and dendrites. (d) EDX analysis of AgCd alloy electro-catalyst deposited on carbon paper.....	93
Figure 5.3 (a) SEM image, and (b) to (d) SEM elemental mapping of AgCd electro-catalyst on the same portion of a carbon paper surface.....	94

Figure 5.4 Cyclic voltammetry curves for AgCd electro-catalyst loaded on carbon fibre paper in O ₂ and N ₂ saturated 0.1M KOH solution.....	95
Figure 5.5 Polarization curves for ORR (disk current only) obtained from RRDE measurement on different working electrodes viz. glassy carbon electrode (red), carbon paper (black) and AgCd electrodeposited on CP (green) in O ₂ saturated 0.1M KOH solution.....	96
Figure 5.6 RRDE polarization curve at different rotation rates in 0.1M KOH saturated with O ₂ at 20 mV/s scan rates for (a) disk current and (b) ring current measurements. (c) Number of electron transferred and (d) peroxide yield for the corresponding ORR process.....	97
Figure 5.7 In-situ FTIR studies with the AgCd electro-catalyst (a) in O ₂ saturated; (b) comparison in N ₂ and O ₂ saturated solutions; (c) enlarged portion of (a) corresponding to O-H stretching region and (d) Absorbance vs applied potential plot.....	99
Figure 5.8 Chrono-amperometric plot at a constant bias potential of -0.35 V vs Ag/AgCl in 0.1 M KOH for three hours.....	101
Figure 6.1 (a) XRD pattern, (b) Raman spectra of the as prepared catalyst and (c) enlarged portion from 40 ^o to 50 ^o 2-theta range.....	113
Figure 6.2 SEM and TEM images of (a-b) for bare g-C ₃ N ₄ and (c-d) for Ag/g-C ₃ N ₄ @GO.....	115
Figure 6.3 EDX patterns of (a) pure g-C ₃ N ₄ and (b) Ag/g-C ₃ N ₄ @GO catalyst.....	116

Figure 6.4 EIS spectra of (a) pure g-C ₃ N ₄ , Ag/g-C ₃ N ₄ and Ag/g-C ₃ N ₄ @GO catalyst loaded on GC disc electrode (b) enlarged view of the EIS spectra in the high frequency region.....	117
Figure 6.5 (a) Comparative RDE polarization curves for GO, g-C ₃ N ₄ , Ag/g-C ₃ N ₄ and Ag/g-C ₃ N ₄ @GO composite loaded on GC rotating disc electrode, (b) RDE polarization curves for Ag/g-C ₃ N ₄ @GO composite loaded GCE at varying rotation speeds, (c) Koutecky-Levich plot for the data shown in (b), and (d) Tafel plot for the polarization curves recorded with Ag/g-C ₃ N ₄ @GO catalyst at 1600 rpm.....	118
Figure 6.6 Tafel Plots for exchange current density.....	122
Figure 6.7 (a) Methanol tolerance test on Ag/g-C ₃ N ₄ @GO electrocatalyst modified cathode; (b) Chronoamperometric stability plot for 3 hours at -0.4 V.....	123
Figure 7.1 Fuel Cell driven by in-situ generated fuel from solar water splitting.....	131
Figure 7.2 SEM and TEM images of CoTiO ₃	132

List of Tables

Table 3.1 EDX compositional analysis of of g-C ₃ N ₄ , Ni-g-C ₃ N ₄ , and Ag/g-C ₃ N ₄ and AgNi/g-C ₃ N ₄	57
Table 3.2 Photocurrent density per mg of metal loading.....	58
Table 6.1 Tafel Analysis for Tafel slope and transfer coefficient.....	121
Table 6.2 Tafel Analysis for exchange current density values that are given in Table 6.1.....	121
Table 6.3 Literature reported Ag based ORR catalyst.....	124

LIST OF ABBREVIATIONS AND SYMBOLS

E_F	Fermi level (in V)
E_g	Bandgap energy (in eV)
E_{Redox}	Redox potential or electrolyte energy mediator (in V)
JCPDS	Joint committee on powder diffraction standards
ϵ_0	Permittivity of free space (= 8.85419×10^{-12} F m ⁻¹)
ϵ	Dielectric constant
EIS	Electrochemical impedance spectroscopy
EDX	Energy Dispersive X-Ray
FESEM	Field emission scanning electron microscopy
FT-IR	Fourier transformed infrared
FTO	Fluorine-doped tin oxide
ITO	Indium-doped tin oxide
LSV	Linear sweep voltammetry
CV	Cyclic Voltammetry
RDE	Rotating Disk Electrode
RRDE	Rotating Ring Disk Electrode
λ	Wavelength (in nm)
MS	Mott–Schottky
NHE	Normal Hydrogen Electrode
N_d	Donor density
PL	Photoluminescence
Pt	Platinum
Ag	Silver
PEC	Photoelectrochemical
SPR	Surface plasmon resonance
SEM	Scanning electron microscopy
T	Temperature (in K or °C)

TEM	Transmission electron microscopy
UV-VIS	Ultraviolet visible
XRD	X-ray diffraction
XPS	X-ray photo spectroscopy
CP	Carbon paper
EDX	Elemental Dispersive X-ray Spectra
GCE	Glassy carbon electrode
GO	Graphene Oxide